5. Net sea-air CO_2 flux estimation

5.1. Computational method for estimating CO_2 flux

The net sea-air CO_2 flux (F_{CO_2}) can be estimated using Eq. 18:

$$F_{CO_2} = K \cdot \Delta p\mathrm{CO_2} \tag{18}$$

In this equation, K is the gas transfer coefficient and $\Delta p\mathrm{CO_2}$ is the difference in $p\mathrm{CO_2}$ between sea and air (=$p\mathrm{CO_2}$s − $p\mathrm{CO_2}$a). K is the product of the gas transfer velocity (k) and the solubility of CO_2 in seawater (L). k is calculated by the method of Wanninkhof (1992), which uses monthly U_{10} values. L is based on the equation of Weiss (1974).

5.2. Seasonal average and variation of CO_2 flux

The 25-year mean monthly CO_2 flux maps for February, May, August and November show the typical horizontal distribution of the CO_2 flux from 1985 to 2009 (Fig. 7). In the equatorial region, $p\mathrm{CO_2}$s is larger than $p\mathrm{CO_2}$a throughout the year, and this region is a major CO_2 source for the atmosphere. This is because of the inorganic carbon supplied from the deeper oceanic layers through equatorial upwelling.

In the subtropical region, because biological CO_2 consumption is low and the mixed layer is shallow, $p\mathrm{CO_2}$s varies with SST because of the thermodynamic effect. $p\mathrm{CO_2}$s is therefore the highest when SST is the highest during summer in each hemisphere and CO_2 uptake in summer is less than in winter. In the North Pacific, $p\mathrm{CO_2}$s in the western region and the coastal region off California is higher than in the other regions. The western region is affected by the Kuroshio and the coastal region off California is influenced by subarctic seawater rich in carbon. The region east of Hawaii is located in the marginal zone between subtropical warm water and subarctic cold water rich in carbon and nutrients; the subtropical water is cooled by the subarctic water and carbon is consumed through biological activity. As a result, $p\mathrm{CO_2}$s in this region is relatively low. However, $p\mathrm{CO_2}$s increases from west to east in the South Pacific. The coastal region off Peru in particular is influenced by coastal upwelling and emits CO_2 to the atmosphere.

In the subpolar regions, $p\mathrm{CO_2}$s is the highest in winter because vertical mixing supplies carbon-rich water from lower layers. In the region east of Japan and in the antarctic region, $p\mathrm{CO_2}$s decreases from spring to summer when phytoplankton consumes CO_2.

The marginal zone between the subtropical and subarctic regions in the Pacific is a major CO_2 sink. Because SST decreases and seasonal wind intensifies in winter, $p\mathrm{CO_2}$s decreases from the thermodynamic effect and the gas transfer coefficient increases. As a result, CO_2 uptake is highest in winter.

Larger standard deviations of CO_2 flux are seen around the equatorial region and the boundary between the subtropical and subpolar regions (Fig. 8). $p\mathrm{CO_2}$s in the equatorial region is affected by ENSO, as mentioned in Section 4. The ENSO cycle affects $p\mathrm{CO_2}$s and wind patterns, causing variations in the CO_2 flux. In the North Pacific boundary region, SST and SLP variations caused by the PDO are predominant. The PDO could affect $p\mathrm{CO_2}$s or U_{10} (and the gas transfer velocity) through anomalies in SST and SLP.

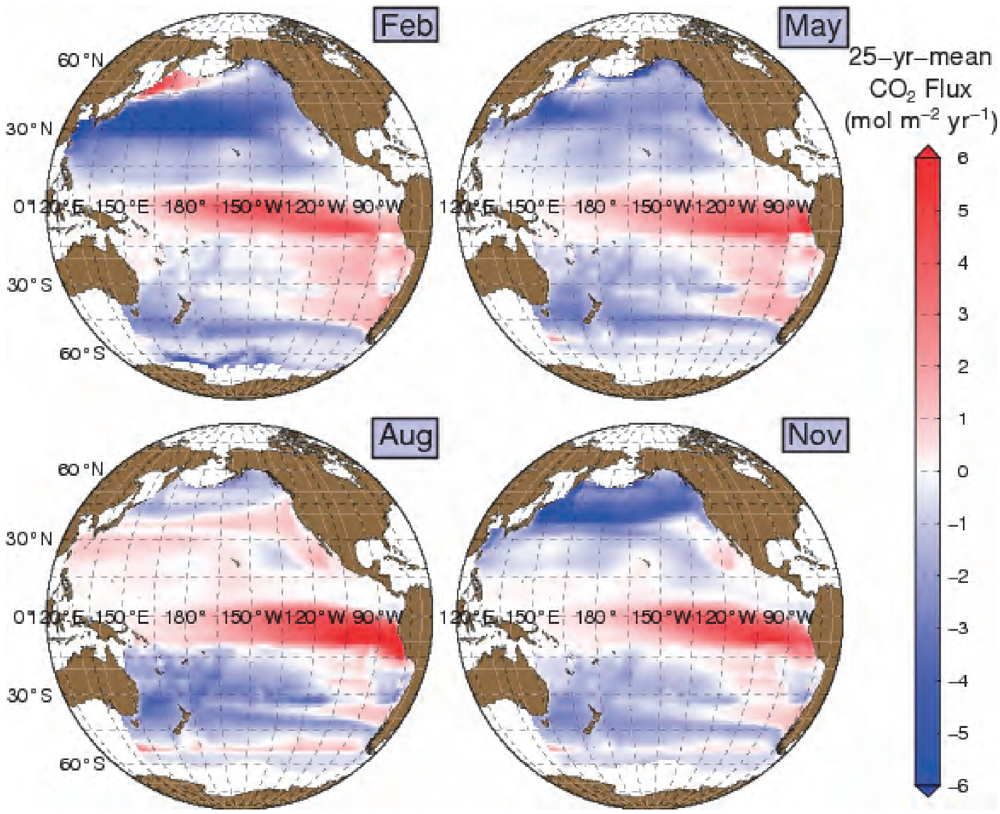

Figure 7. Monthly mean CO_2 flux maps for February, May, August and November. The color scale shows the level of CO_2 source or sink.

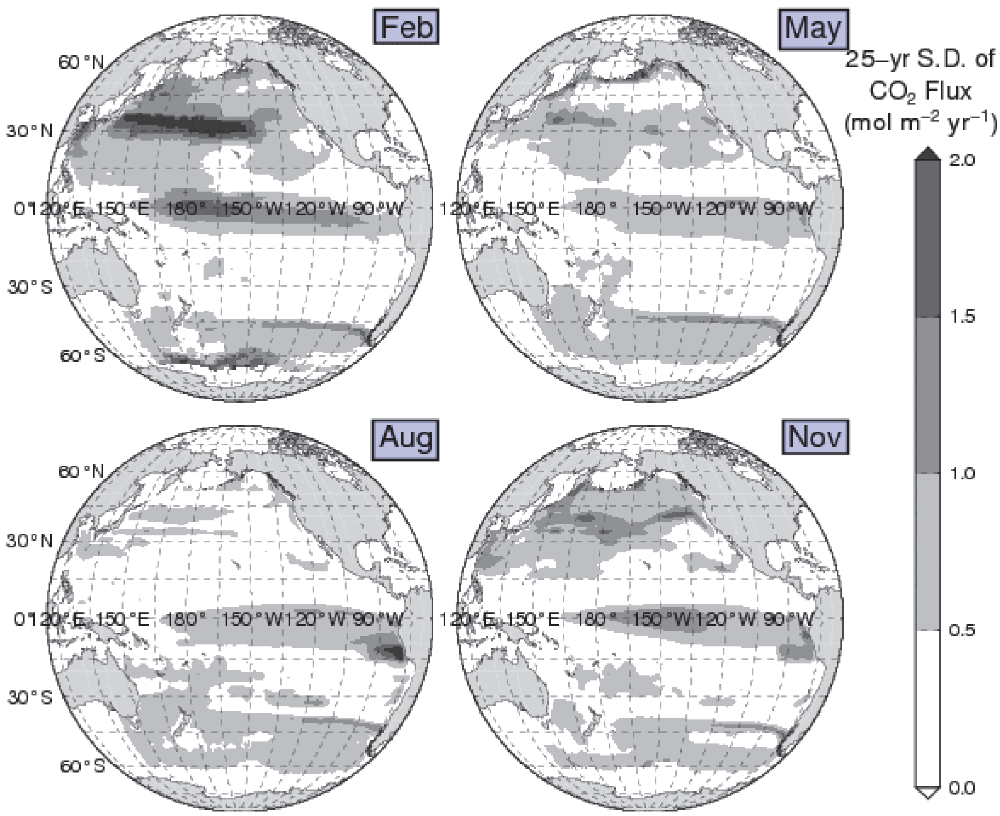

Figure 8. Standard deviations of monthly CO_2 flux (mol m^{-2} yr^{-1}) in February, May, August and November.

5.3. Time series of area-integrated CO_2 flux

We calculated the area-integrated monthly and annual CO_2 flux from 1985 through 2009 (Fig. 9). In the equatorial region, CO_2 outgassing varies with ENSO. CO_2 emission decreases during El Niño periods (ENSO warm phase) and increases for La Niña periods (ENSO cold phase). For the 1997/1998 El Niño period in particular, CO_2 emission was 70% of that during normal periods.

In contrast, seasonal variation predominates in the subtropical regions, and CO_2 uptake decreases in summer and increases in winter. The amplitude of the variation in CO_2 flux is greater in the northern hemisphere than in the southern. This reflects the larger seasonal SST amplitude and more severe winter winds in the northern hemisphere.

As in the subtropical regions, there is seasonal variation in the subarctic region as well. Unlike the subtropical regions, the CO_2 flux in the subarctic region is at a minimum in spring due to biological uptake of CO_2. There is seasonal variation in CO_2 flux in the subantarctic region, with a maximum uptake by the sea in austral summer and a minimum uptake in austral winter. This is because the amount of inorganic carbon supplied by vertical mixing is small and biological uptake increases in austral summer.

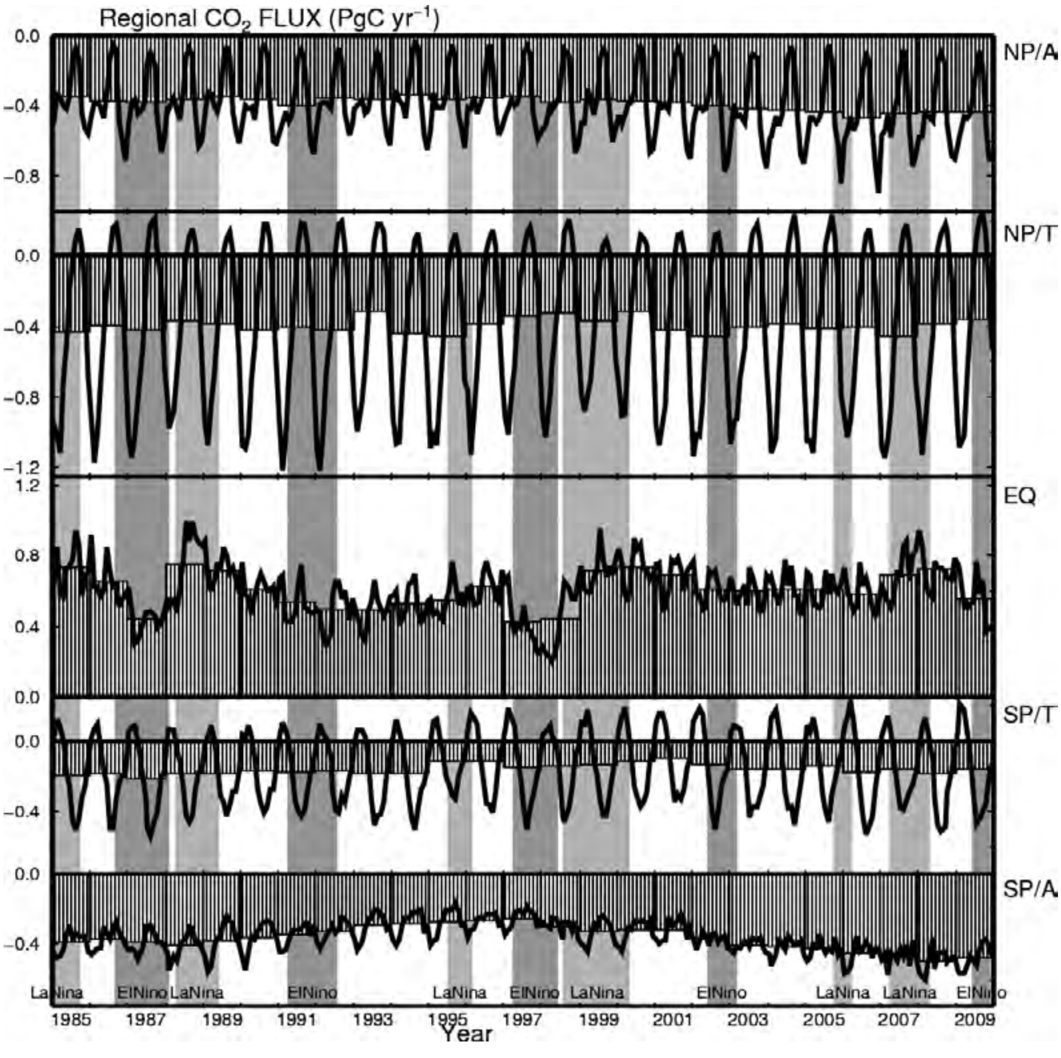

Figure 9. Time series of regional CO_2 flux (PgC yr^{-1}) for the Pacific Ocean. Lines and boxes show monthly and annual CO_2 flux, respectively. Shading indicates ENSO events: dark grey, El-Niño; light grey, La-Niña.

5.4. Comparison with the climatological CO_2 flux

We compared the meridional distribution of the CO_2 flux in 2000 determined in this study with the climatological CO_2 flux for the reference year 2000 as reported by Takahashi et al. (2009b) (Fig. 10). The results of this study correspond qualitatively with the climatology. However in the equatorial region the flux estimated in this study is double the climatological flux estimate.

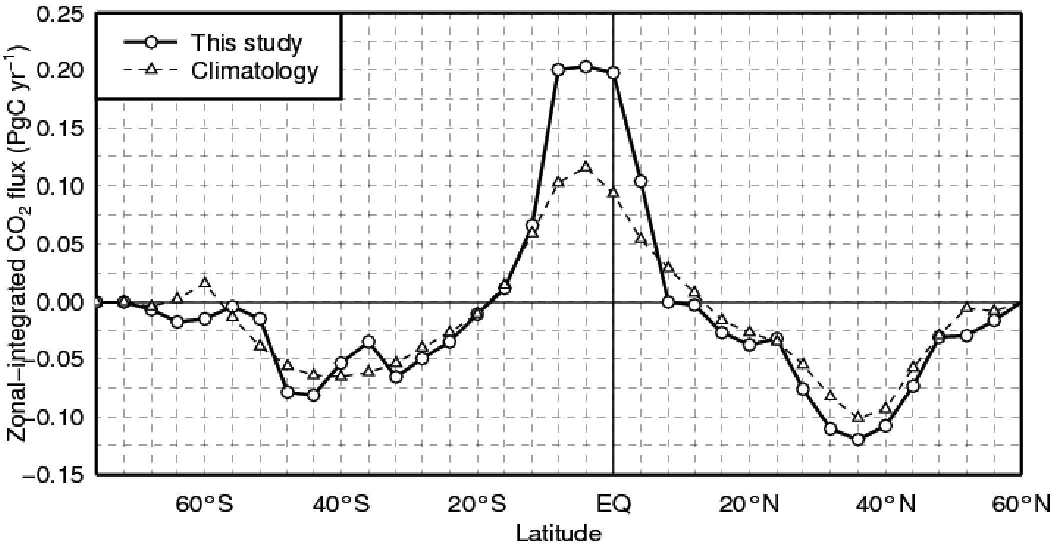

Figure 10. Meridional distribution of the zonally-integrated CO_2 flux (PgC yr^{-1}) in 2000 from this study (solid line) and the climatological CO_2 flux in the reference year 2000 from Takahashi et al. (2009b) (dashed line).

Table 3 presents the comparison between the flux determined in this study and the climatological flux estimate in each zonal band. The absolute values from this study are larger than those of the climatology in all zonal bands. In this study we used different U_{10} analysis data and a different equation for the gas transfer coefficient than used for the climatology data. As a result, the gas transfer coefficients in this study are from about 1.5 to 2 times those of the climatology.

Table 3. Comparison between the CO_2 fluxes estimated in this study and the climatological CO_2 flux in each zonal band. The gas transfer coefficient used in this study is from the equation of Wanninkhof (1992). Positive and negative CO_2 fluxes refer to sea-to-air or air-to-sea transfers of CO_2, respectively. The column "The average values for 1985–2009" is the average and standard deviation of the annual mean CO_2 fluxes between 1985 and 2009.

Zone	This study In 2000 (PgC yr^{-1})	This study Average 1985-2009 (PgC yr^{-1})	Takahashi *et al.* (2009b) (PgC yr^{-1})
N. of 50°N	–0.06	–0.06±0.01	–0.03
14°N-50°N	–0.64	–0.70±0.05	–0.50
14°S-14°N	+0.77	+0.62±0.10	+0.48
50°S-14°S	–0.42	–0.46±0.08	–0.41
Sum.	–0.34	–0.59±0.14	–0.46

Because a La Niña event continued until the spring of 2000, the pCO_2s values in this study, which reflect the real-time oceanic conditions, are larger than the climatological pCO_2s in the equatorial region (Fig. 11). The difference between the CO_2 flux estimates results from the difference in gas transfer coefficient and the La Niña event.

In the Pacific north of 50°S, the mean flux from 1985 through 2009 estimated in this study is −0.59 PgC yr^{-1}; the flux estimate for 2000 is −0.34 PgC yr^{-1} and the climatological flux in the reference year 2000 is −0.46 PgC yr^{-1}. The estimated annual CO_2 flux in 2000 from this study is smaller uptake than the climatological estimate because of the influence of La Niña. The mean annual flux from this study is larger uptake than the climatological flux estimate because of the difference in the gas transfer coefficients.

The surface of the Pacific Ocean accounts about 46% of the ocean surface worldwide. However, the average CO_2 uptake in the Pacific as estimated in this study is about 32% of the total absorption by the Global Ocean (2.2 PgC yr^{-1}; IPCC, 2007). The proportional CO_2 uptake in the Pacific Ocean is smaller than the proportional area because of the Pacific equatorial region, which is the area of greatest CO_2 release in the world.

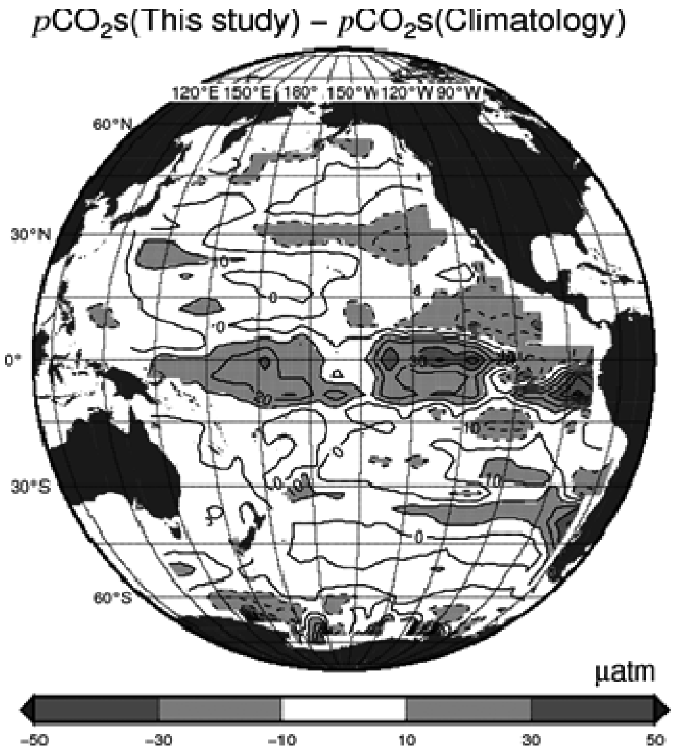

Figure 11. Mean difference between the pCO_2s values in 2000 estimated in this study and the climatological pCO_2s values (Takahashi et al., 2009b). The difference is defined as the value from this study minus the climatological value.

5.5. Effects of gas transfer coefficient equations on CO_2 flux

We used the formula of Wanninkhof (1992; hereafter "W92") to estimate CO_2 flux. In other recent studies, other formulas have been proposed, such as those of Nightingale et al. (2000; hereafter "N00") and Sweeney et al. (2007; hereafter "S07"). We compared the CO_2 fluxes estimated using gas transfer coefficients calculated using these three formulas. The results of this comparison are summarized in Table 4. Absolute value of annual mean CO_2 flux estimates based on N00 using JRA25/JCDAS wind speed fields were the lowest and those using W92 were the highest. In each region, the difference between gas transfer coefficients is 15–20%. This difference is comparable to the uncertainty in the gas transfer coefficients of about 30% (Sweeney et al., 2007).

5.6. Effect of wind speed on CO_2 flux

To calculate gas transfer coefficients we used not only the wind velocity fields from JRA25/JCDAS but also those from National Centers for Environmental Prediction / National Center for Atmospheric Research (NCEP/NCAR) Reanalysis I (Kalnay et al., 1996; hereinafter CDAS1) and from a cross-calibrated, multi-platform (CCMP), multi-instrument ocean surface wind velocity data set (Ardizzone et al., 2009). We used SLP fields from JRA25/JCDAS because the mean SLP difference between JRA25/JCDAS and CDAS1 is about 1 hPa and this results in a difference in pCO$_2$s of only 0.1% (0.4 μatm). The effect of the SLP difference is less than the pCO$_2$s estimation error of −10 to +10 μatm.

In Table 4, we summarize the annual regional CO_2 flux as estimated using three different types of U_{10} data. Except for the equatorial region (14°S–14°N), the CO_2 flux estimates agree with each other. In the equatorial region, CO_2 emission based on CDAS1 is the smallest among the three wind velocity fields. For example, the difference in CO_2 flux estimates based on the JRA25/JCDAS and CDAS1 U_{10} fields using the W92 equation is about 20% (0.12 PgC yr^{-1}). This is because the U_{10} of CDAS1 is 10% weaker than that of JRA25/JCDAS due to the differences of models and assimilated datasets. When the gap between U_{10} values is 10%, that between gas transfer coefficients accounts for about 20% of the difference because the gas transfer coefficient is proportional to the square of U_{10}. For the entire Pacific Ocean, estimates using JRA25/JCDAS show lower CO_2 uptake than those using CDAS1 because of higher CO_2 emission in the equatorial region.

Table 4. Comparison of different estimates of the CO_2 flux (PgC yr^{-1}) for each zonal band using equations for gas transfer coefficients from three sources — Wanninkhof (1992; W92), Nightingale et al. (2000; N00) and Sweeney et al. (2007; S07) — and U_{10} fields from JRA25/JCDAS, NCEP/NCAR Reanalysis I, and a cross-calibrated, multi-platform (CCMP) dataset. Values for CO_2 flux are means and standard deviations from 1985 through 2009 (1990–2009 for CCMP).

	Gas transfer velocity	JRA25/JCDAS	CDAS1	CCMP	Clim
N. of 50N	W92	-0.06 ± 0.01	-0.07 ± 0.01	-0.06 ± 0.01	
	N00	-0.05 ± 0.01	-0.05 ± 0.01	-0.05 ± 0.01	*-0.03*
	S07	-0.05 ± 0.01	-0.06 ± 0.01	-0.05 ± 0.01	
14N-50N	W92	-0.70 ± 0.05	-0.70 ± 0.04	-0.75 ± 0.05	
	N00	-0.51 ± 0.03	-0.51 ± 0.03	-0.53 ± 0.03	*-0.50*
	S07	-0.56 ± 0.03	-0.56 ± 0.03	-0.55 ± 0.03	
14S-14N	W92	0.62 ± 0.10	0.50 ± 0.07	0.68 ± 0.09	
	N00	0.44 ± 0.06	0.37 ± 0.05	0.48 ± 0.06	*0.48*
	S07	0.45 ± 0.07	0.37 ± 0.05	0.46 ± 0.06	
50S-14S	W92	-0.46 ± 0.08	-0.48 ± 0.07	-0.52 ± 0.07	
	N00	-0.34 ± 0.05	-0.35 ± 0.05	-0.37 ± 0.05	*-0.41*
	S07	-0.37 ± 0.06	-0.38 ± 0.05	-0.39 ± 0.05	
S. of 50S	W92	-0.11 ± 0.04	-0.10 ± 0.03	-0.09 ± 0.02	
	N00	-0.08 ± 0.03	-0.07 ± 0.03	-0.06 ± 0.02	-
	S07	-0.09 ± 0.04	-0.08 ± 0.03	-0.07 ± 0.02	
Pacific	W92	-0.70 ± 0.14	-0.84 ± 0.11	-0.74 ± 0.14	
	N00	-0.53 ± 0.10	-0.62 ± 0.08	-0.54 ± 0.10	-
	S07	-0.62 ± 0.10	-0.71 ± 0.09	-0.59 ± 0.10	